Motion Prediction Envelopes for Intact and Damaged Hulls

Leigh S. McCue

Virginia Tech

ABSTRACT

In this work, the author uses past ship motion histories to provide an envelope of predicted future motions. By using past motion information to serve as an indicator of likely future motion, in essence, we are assuming that when a ship is in a given roll/pitch configuration, some relatively deterministic sequence of events put it into that configuration with subsequent behavior falling within an envelope of motions. The simple and computationally efficient method is applied to both intact and damaged experimental data in regular and random seas respectively. This information can be used both to anticipate future motions and to highlight deviations from expected motions indicating changing behaviour due to damage and/or flooding.

KEYWORDS

Ship motion prediction; motion envelope; intact stability; damaged stability

INTRODUCTION

"The leading cause of fatalities in the commercial fishing industry is drowning due to the loss of a fishing vessel" (Lincoln, 2007). Between 1994 and 2004, 641 commercial fishermen died in the United States, 328 (51%) due to vessel flooding/sinking/capsize (Dickey and Ellis, 2006). In the United States in 2006, 51 fishers and related fishing workers were killed on the job. This yields an occupational mortality rate of 141.7 for every 100,000 workers, highest of all occupations in the United States and over 36 times higher than the mortality rate for the average U.S. worker (Bureau of Labor Statistics, 2007).

The aim of this work is to predict an envelope of ship motions without *a priori* information as to the oncoming seas. While simulation tools allow for populating a database of predicted ship motions in both intact and damaged scenarios, most notably as developed in the Orpheus system (QinetiQ, 2006), for small and/or one-off ships, like many fishing vessels, such a computationally intensive procedure is likely prohibitively expensive. Similarly, expecting small craft to have an accurate means of measuring oncoming waves such as WaMoS II (Reichert *et al.*, 2005) is perhaps unrealistic. This work seeks to develop affordable tools readily deployed to variety of unique vessels. Therefore, we will rely on past and current ship behaviour to provide future hazard warnings.

In this study two sets of experimental data are used. Data from seakeeping tests of a 1/46.6th scale notional destroyer model, DTMB Hull 5514, in regular seas is used as the intact ship case (Hayden *et al.*, 2006). A 1/40th scale model test of a passenger Ro-Ro vessel in beam seas dictated by a JONSWAP spectrum is used as the damaged stability case (Jasionowski *et al*, 2003). While both models represent ships far from a fishing vessel, they are sufficiently different to illustrate the generality of this approach.

DETERMINISM

The methodology outlined in the next section relies upon an assumption of the ship's roll and pitch behaviour having deterministic characteristics. To identify if there is structure, fundamentally, to the time series data to justify proceeding along the planned approach, the author investigated recurrence plots of the subsets of the time series data. A recurrence plot is a pictorial representation of neighboring points in phase space (Kantz & Schreiber, 2004). That is, if the state of the vessel at time *j* is close to that of time *i*, the point *j* is considered a neighbor and marked with a dot at (*i, j*) on a recurrence plot. For this work, the state variables used in the determination were roll, ϕ, pitch, θ, roll velocity, and pitch velocity. Velocities were included to give weight to direction of motion in addition to magnitude in finding neighbors. Each variable was normalized by its standard deviation, such that each is equally important in the determination of neighbors. Examining sample intact DTMB hull 5514 and damage Ro-Ro time histories, Figures 1(a) and (b) show recurrence plots for (*i,j*) pairs meeting the criteria in Equation 1 for ε=0.25 and 0.2. Figures 1(c) and (d) give correlation integral as a function of ε. Correlation integral is the fraction of (*i,j*) pairs in a recurrence plot (Kaplan & Glass, 1995).

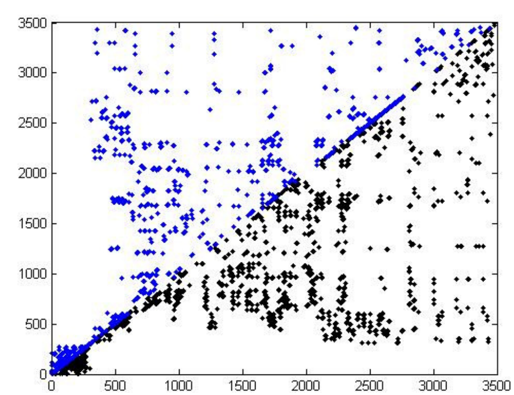

Fig. 1(a): Recurrence plot for DTMB5514 case 212, ε=.25 below the diagonal, ε=.2 above the diagonal.

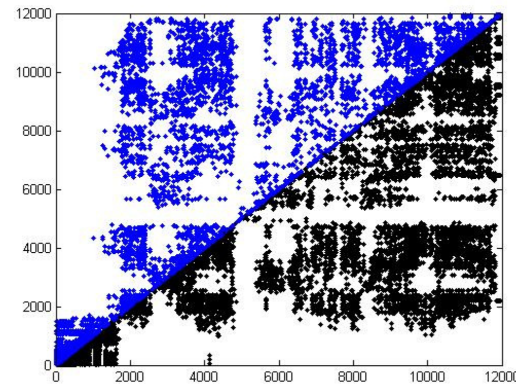

Fig. 1(b): Recurrence plot for Ro-Ro case 101, ε=.25 below the diagonal, ε=.2 above the diagonal.

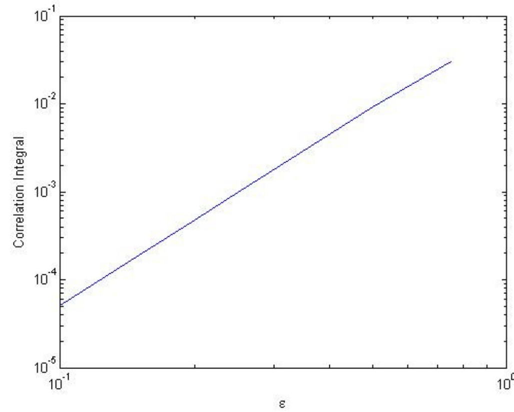

Fig. 1(c): Correlation integral versus ε for DTMB5514 case 212.

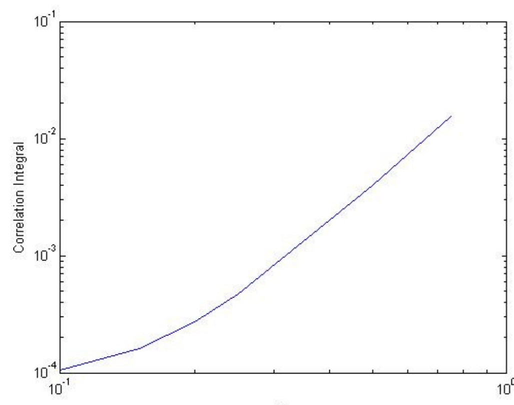

Fig. 1(d): Correlation integral versus ε for Ro-Ro case 101.

$$\| \left\langle \phi/\sigma_{\phi}, \theta/\sigma_{\theta}, \dot{\phi}/\sigma_{\dot{\phi}}, \dot{\theta}/\sigma_{\dot{\theta}} \right\rangle_i - \left\langle \phi/\sigma_{\phi}, \theta/\sigma_{\theta}, \dot{\phi}/\sigma_{\dot{\phi}}, \dot{\theta}/\sigma_{\dot{\theta}} \right\rangle_j \| < \varepsilon \qquad (1)$$

There is structure to this data, although it is not simply periodic. This is likely due to the irregularity of the wave excitation. Obviously, the stronger the determinism in the system, the easier prediction would be.

METHODOLOGY

To generate estimates of oncoming time series, we shall assume the data to be at least minimally deterministic and thus capitalize upon the information contained in nearest neighbours to the point of interest. The procedure is outlined as follows:

1. Input roll, pitch, roll velocity, and pitch velocity past time history and non-dimensionalize with each variables standard deviation.
2. Search non-dimensional past time history for *n* neighbours nearest to the point of interest (point of interest being the time from which we wish to approximate forward, and *n* for this work was selected as 10). Additionally, immediate neighbours in time are not selected as state-space neighbours; that is, each neighbour is checked to the time step immediately before and after to verify that it is the closest neighbour of the three. This is to keep from selecting multiple neighbours that are all part of the same roll/pitch event.
3. Note the actual dimensional roll, pitch, roll velocity and pitch velocity trajectories for the duration of interest immediately following each of the 10 nearest neighbours.
4. Generate 1, 2, and 3 standard deviation (1, 2, 3σ) envelope curves of predicted motions based upon the mean value ±1, 2, 3σ at each time step from the neighbour time histories. That is, use the time series immediately following each of the *n* nearest neighbours as an estimate of the behaviour immediately following the point of interest.

INTACT CASE (DTMB HULL 5514)

Beginning with non-capsize DTMB hull 5514 case 212 for ship motions at $Fn=0.20$ in stern-quartering seas at $\lambda/L\approx.75$ and $H/\lambda\approx1/10$, in Figure 2(a)-(f) we see that this approach yields accurate roll and pitch envelope predictions for the first few cycles with accuracy diminishing as we progress further in time. Despite the hull 5514 experiments being conducted in simulated regular waves, the response is not purely sinusoidal. This is primarily driven by variations in generating such large model scale waves and because the ship is nominally at the specified Froude number and heading, although it gets pushed off heading/speed to some extent as a result of the large waves.

Note, the goal of this is not to precisely predict the vessel time history, but rather to provide an envelope of anticipated motions. Therefore, over-prediction is not deemed a bad thing—rather the amount of desired margin can be adjusted by adjustment of the envelope size (that is, 1σ, 2σ, 3σ, etc…). 1σ envelopes of roll and pitch motions are presented in Figures 2(a) and 2(b) respectively. Throughout the rest of this work, the 1σ envelope will be used, however, for reference in this sample DTMB5514 case 212, 2σ and 3σ envelopes of roll and pitch motions are given in Figures 2(c)-(f).

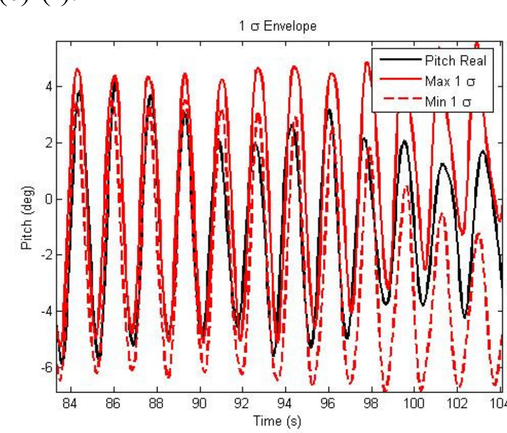

Fig. 2(a): Predicted roll envelope (1σ) versus actual time history for DTMB5514 case 212.

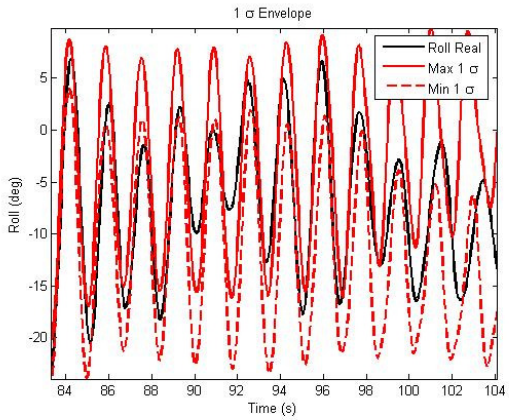

Fig. 2(b): Predicted pitch envelope (1σ) versus actual time history for DTMB5514 case 212.

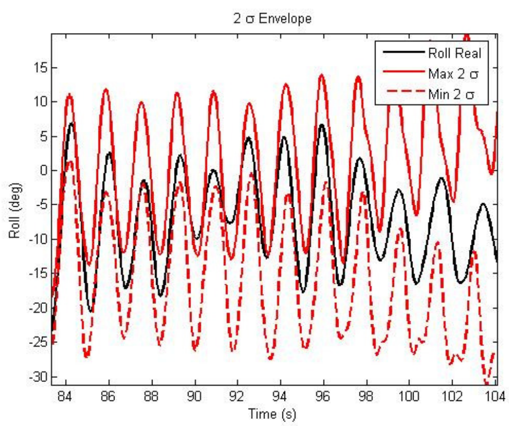

Fig. 2(c): Predicted roll envelope (2σ) versus actual time history for DTMB5514 case 212.

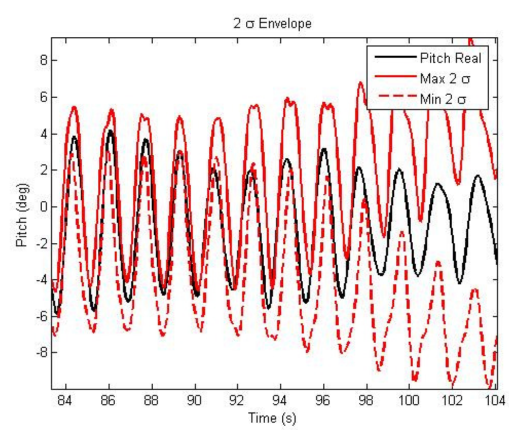

Fig. 2(d): Predicted pitch envelope (2σ) versus actual time history for DTMB5514 case 212.

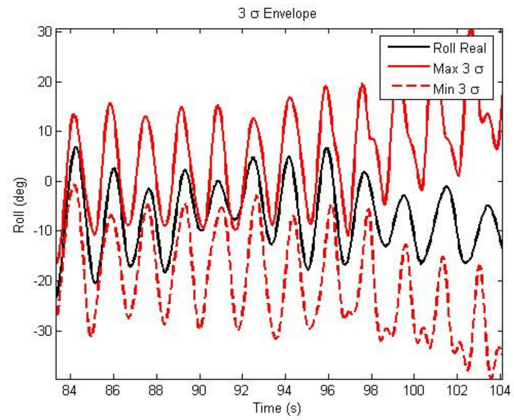

Fig. 2(e): Predicted roll envelope (3σ) versus actual time history for DTMB5514 case 212.

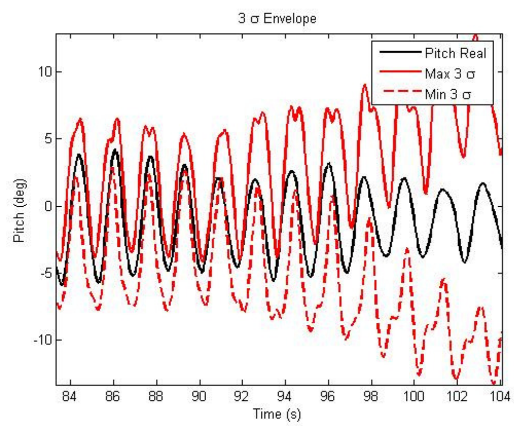

Fig. 2(f): Predicted pitch envelope (3σ) versus actual time history for DTMB5514 case 212.

Table 1: Parameters for DTMB5514 case 212 roll data and max/min envelope predictions

Data	Mean (deg)	Standard Deviation (deg)
Roll—entire series	-6.15	7.20
Roll—segment	-7.10	6.77
+1σ envelope	-3.29	8.19
-1σ envelope	-11.98	8.07

Statistics for DTMB5514 case 212 shown in Figure 2 are summarized in Table 1. Specifically, mean and standard deviation are given for the entire roll time series, for actual roll motions during the period of time shown in Figure 2(a), and for the ±1σ bounds of Figure 2(a). The envelope bounds are less restrictive and clearly less arbitrary than defining bounds based purely on a standard deviation from the mean roll values.

For the sake of comparison, and to demonstrate repeatability, this approach is used for the same window of time for DTMB5514 case 323. Case 323 is a non-capsize run at $Fn=0.10$ in stern-quartering seas with $\lambda/L=1.244$ and $H/\lambda\approx1/10.392$. Case 323 features significantly larger roll motions than Case 212. Figures 3(a) and (b) show predicted roll and pitch 1σ envelopes as compared to actual motions.

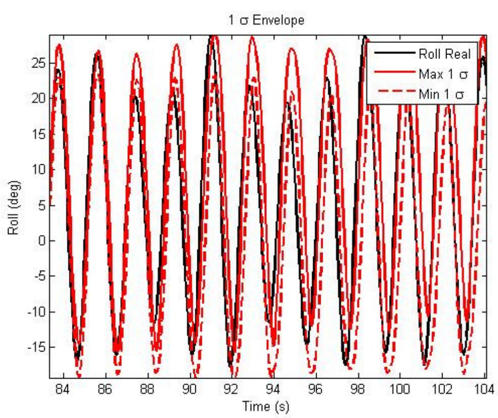

Fig. 3(a): Predicted roll envelope (1σ) versus actual time history for DTMB5514 case 323.

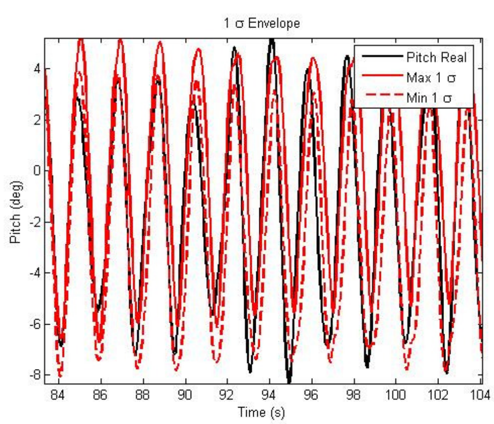

Fig. 3(b): Predicted pitch envelope (1σ) versus actual time history for DTMB5514 case 323.

Corresponding statistics for case 323 are presented in Table 2, in which we again note that this approach is less restrictive than defining an arbitrary limit based upon the statistics of the entire time history while still accurately providing an estimated bound to future ship motions.

Table 2: Parameters for DTMB5514 case 323 roll data and max/min envelope predictions

Data	Mean (deg)	Standard Deviation (deg)
Roll—entire series	3.57	13.84
Roll—segment	4.95	14.32
+1σ envelope	9.29	14.61
-1σ envelope	-0.09	14.43

In this work, non-capsize runs at relatively low speed were used to provide a longer time history from which to find neighbours. A capsize case is presented in the following section on damaged stability.

DAMAGED CASE (RO-RO MODEL)

To illustrate the generality of this method, and its application under extreme circumstances, such as flooding or capsize, we shall apply it to sample time histories from a damaged Ro-Ro model test. Unlike the DTMB5514 tests, conducted in regular seas, the tests generating the data used herein were conducted in random beam seas modelled by a JONSWAP spectrum (Jasionowski *et al.*, 2003).

Consider, for example, Ro-Ro model test number 101. The roll history reaches a maximal value at time 1083.2s. Applying the same methodology to ‘predict’ forward from time 948.7s to 1054.1s in Figures 4(a) and 4(b) we note the onset of odd behaviour well outside the 1σ window as we approach this maximum roll condition.

While the initial 1-2 roll cycles yield very good agreement between actual and predicted motions, by time 1010s motions well outside the predicted range are observed. Clearly we expect the prediction to grow worse as we move forward in time, but the deviations in roll occurring between times 1010-1020s are sufficiently severe to call attention to the behaviour occurring prior to the maximum value which occurs over 60 seconds later. This information could be used to indicate to the captain that his vessel's behaviour is outside the anticipated and thus he should proceed with caution and trouble-shoot appropriately (*i.e.*, seek out possible sources of flooding).

Similarly, examining the period immediately proceeding capsize (at time 1994s) in model test number 400 we observe a distinct deviation from the predicted 1σ motions minutes before capsize. At approximately time 1860s, we observe an entire roll cycle outside the predicted envelope as shown in Figure 5(a). Additionally, there is a large pitch deviation as a precursor to the capsize event, Figure 5(b). These types of deviation from the predicted envelope curves would serve as an advance warning.

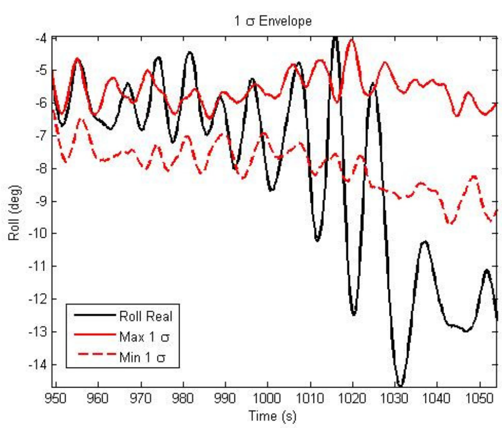

Fig. 4(a): Predicted roll envelope (1σ) versus actual time history for Ro-Ro case 101.

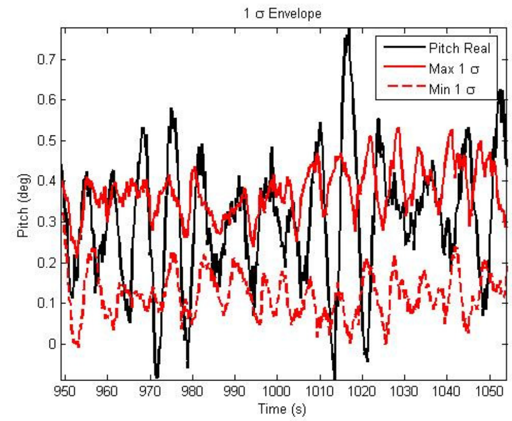

Fig. 4(b): Predicted pitch envelope (1σ) versus actual time history for Ro-Ro case 101.

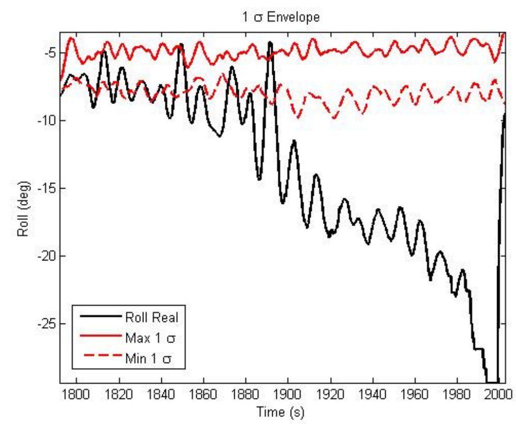

Fig. 5(a): Predicted roll envelope (1σ) versus actual time history for Ro-Ro case 400.

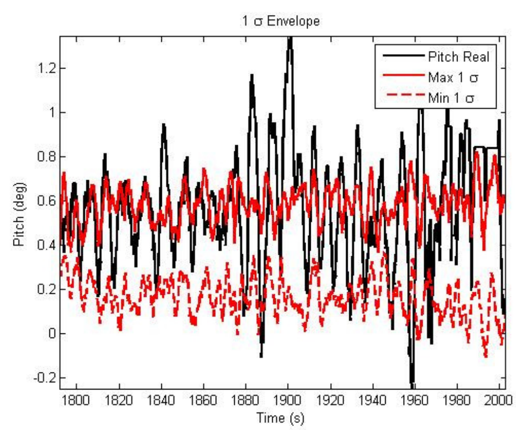

Fig. 5(b): Predicted pitch envelope (1σ) versus actual time history for Ro-Ro case 400.

ON THE NATURE OF THE DATA FIT

Both the DTMB Hull 5514 capsize tests and the damaged Ro-Ro vessel data exhibits strongly nonlinear behaviour. Following the work of Belenky (1994) and Haddara and Zhang (1994) and summarized in the text by Belenky and Sevastianov (2007), for these data sets a Gaussian distribution yields a relatively poor representation of the roll process while the PDF in Equation (2) generated using the Gram-Charlier A series more accurately represents the roll probability density function.

$$f(x) = \frac{1}{\sigma\sqrt{2\pi}} \exp\left(-\frac{(x-\mu)^2}{2\sigma^2}\right) \cdot \left(1 + \frac{\kappa_3}{\sigma^3 3!} H_3\left(\frac{x-\mu}{\sigma}\right) + \frac{\kappa_4}{\sigma^4 4!} H_4\left(\frac{x-\mu}{\sigma}\right)\right) \quad (2)$$

In Equation (2), $H_n(x)$ are Hermite polynomials defined in Equation (3) and κ_n are the nth cumulants of the data set.

$$H_n(x) = (-1)^n \exp\left(\frac{x^2}{2}\right) \frac{d^n}{dx^n}\left(\exp\left(\frac{-x^2}{2}\right)\right) \quad (3)$$

Focusing, for example on the damaged Ro-Ro case 101, Figure 6(a) shows the entire raw roll data fit by both a Gaussian and Gram-Charlier series.

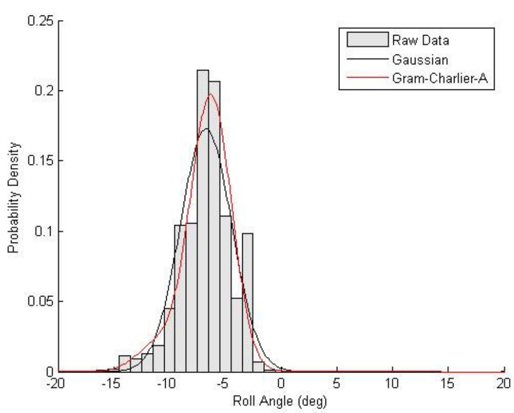

Fig. 6(a): Ro-Ro case 101 raw roll data fit with Gaussian and Gram-Charlier distributions.

The skewness, $\kappa_3/\kappa_2^{3/2}$, and excess kurtosis, κ_4/κ_2^2 (Williams, 2001, Belenky and Sevastianov, 2007), of this fit are -0.60 and 0.92 respectively.

In figure 6(b) a similar probability density function comparison is shown for the Ro-Ro capsize case 400 from time zero up to the time of the start of Figure 5 (*i*.e. t=1792.1s—to illustrate time history behaviour prior to capsize). The skewness and kurtosis of this data set are -1.08 and 1.17 respectively.

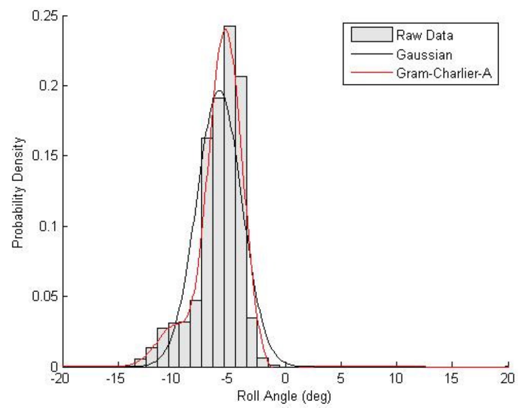

Fig. 6(b): Ro-Ro case 400 roll data (t=0-1792.1) fit with Gaussian and Gram-Charlier distributions.

With this information, as a topic for further research, one may opt to consider revising the previously described approach to apply a more sophisticated envelope formulation employing the skewness and kurtosis of the data.

CONCLUSIONS

This approach is obviously limited by a lack of knowledge of the oncoming waves, and to a lesser extent the wind environment. A single atypical wave could dramatically alter the vessel responses in a manner that cannot be predicted using this formulation. The behaviour is not sinusoidal, nor is it even ideally deterministic, without knowledge of the forcing waves and wind. The bounds presented purely reflect typical behaviour of the ship when it has previously been in a similar state. It does not give any guarantee that motions will not exceed that indicated by the various boundaries provided.

That said, the results presented show that it is feasible to anticipate some typical range of motions in a general manner with fair reliability. Since an amount of time equal to the desired duration of prediction following any neighbour is required, we are unable to use that duration worth of data immediately proceeding the point of interest, data which is likely most statistically similar to the actual point of interest. Yet, this approach would only improve with longer durations of data, as this will allow for more, better, neighbours. As a real-time monitoring system where database size would be limited only by computational power and data storage capabilities, hours, if not days, of data could, and should be used.

To optimize this as an on-board tool, further assessment, specifically tailoring the conservatism of the envelope bounds to the needs of the customer, based both on tolerance to both motions under-prediction and over-conservatism. Certainly improvements in this method may also be viable by further investigation into the normalization or relative weighting of the roll, pitch, roll velocity, and pitch velocity data, inclusion of other state variables, and/or improvements in the statistical modeling. Additionally, it would be interesting to study how this compares with other approaches including, but not limited to, Kalman filtering and neural network/learning based algorithms. Further work could also include development of a neural network which outputs this form of envelop bounds, rather than specific expected time history. Repeating this form of analysis with input wave information is likely to improve results whilst also increasing computation time.

ACKNOWLEDMENTS

The author wishes to thank Dan Hayden for his work in reducing and documenting the DTMB Model 5514 experimental data, William Belknap for sharing the 5514 data, Andrzej Jasionowski for providing the damaged ship data, and both Jennifer Lincoln and Gabriele Bulian for their insightful discussions. This work has been supported in part by ONR Grant N000140610551.

REFERENCES

Bureau of Labor Statistics, "Selected occupations with high fatality rates, 2006," at http://www.bls.gov/iif/oshwc/cfoi/cfch0005.pdf, 2007.

Belenky, V., "Piece-wise linear methods for the probabilistic stability assessment for ship in a seaway," *5th International Conference on Stability of Ships and Ocean Vehicles (STAB'94)*, Florida Institute of Technology, Melbourne, Florida, November, 1994.

Belenky, V. and Sevastianov, N.B., *Stability and Safety of Ships: Risk of Capsizing, 2nd Edition*, Jersey City, NJ: Society of Naval Architects and Marine Engineers, 2007.

Dickey, D. and Ellis, LT Q.P., "Analysis of fishing vessel casualties, a review of lost fishing vessels and crew fatalities, 1994-2004," at http://www.uscg.mil/hq/g-m/moa/docs/fvstudy9404.pdf, 2006.

Hayden, D., Bishop, R., Park, J., and Laverty, S., "Model 5514 capsize experiments representing the pre-contract DDG51 hull form at end of service life conditions," Naval Surface Warfare Center Carderock Division, Ship Hydromechanics Department, Bethesda, MD, 2006.

Haddara, M.R. and Zhang, Y., "On the joint probability density function of non-linear rolling motion," *Journal of Sound and Vibration*, **169**(4), 1994, pp. 562-569.

Jasionowski, A., Vassalos, D., and Guarin, L., "Time-based survival criteria for passenger Ro-Ro vessels," *Marine Technology*, Volume 40, Number 4, October 2003, pp. 278-287.

Kaplan, D. and Glass, L., *Understanding Nonlinear Dynamics*, New York: Springer-Verlag, 1995.

Kantz, H. and Schreiber, T., *Nonlinear Time Series Analysis, Second Edition*, Cambridge: Cambridge University Press, 2004.

Lincoln, J., "Commercial Fishing Vessel Safety," statement to the Committee on Transportation and Infrastructure Subcommittee on Coast Guard and Maritime Transportation, United States House of Representatives, 2007.

QinetiQ, "Orpheus-Data Sheet," at http://www.qinetiq.com/home/defence/technology_solutions/maritime/downloads/cl_and_ds.Par.83760.File.pdf, 2006.

Reichert, K., Hessner, K., Dannenberg, J., Trankmann, I., and Lund, B., "X-band radar as a tool to determine spectral and single wave properties," *Fifth International Symposium WAVES 2005*, Madrid, Spain, 2005.

Williams, D., *Weighing the Odds: A Course in Probability and Statistics*, New York: Cambridge University Press, 2001.